Solution Studies of a Water-stable, Trivalent Antimony Pnictogen Bonding Anion Receptor with High Binding Affinities for CN⁻, OCN⁻ and OAc⁻.

Jinchun Qiu, ^{†a} Curt N. Bateman, ^{†a} Shuai Lu, ^b Gary C. George III, ^a Xiaopeng Li, ^b John D. Gorden, ^a Serhii Vasylevskyi ^a and Anthony F. Cozzolino ^a, *

- ^a Department of Chemistry and Biochemistry, Texas Tech University, Box 1061, Lubbock, Texas 79409-1061, United States
- ^b College of Chemistry and Environmental Engineering, Shenzhen University, Shenzhen, Guangdong 518055, China

Supporting Information Placeholder

ABSTRACT: The solution phase anion binding behavior of a water-stable bidentate pnictogen bond donor was studied. A modest change in the visible absorption spectrum allowed for the determination of binding constants. High binding constants were observed with cyanide, cyanate and acetate and these were corroborated with density functional theory (DFT) calculations. The receptor could be recovered free from anion following treatment with methyl triflate, confirming that it remains intact. The tight binding of cyanide and water stability were exploited to use this system as a supramolecular catalyst in a phase-transfer Strecker reaction, further demonstrating the utility of pnictogen bonding as a tool in noncovalent catalysis.

INTRODUCTION

Anion binding and recognition, an important sub-field of hostguest interactions, is used to direct crystal engineering and molecular templating, 1,2 for selective sensing of anions, 3,4 and for metalfree catalysis in organic synthesis.^{5,6} The pnictogens have played an important role in anion binding when in the +5 oxidation state.7-13 This is largely due to the high Lewis acidity of the electron deficient central pnictogen. Pnictogens in the +3 oxidation state are typically viewed as Lewis bases due to the presence of a lone pair.14-17 The heaviest pnictogens are amphoteric in the +3 oxidation state, and by carefully choosing the chemical environment of the pnictogen, the scales can be tipped towards Lewis acidity allowing for anion binding mediated by pnictogens in the +3 oxidation state. 18-25 Figure 1 depicts some of the examples where trivalent pnictogens have been purposefully used for anion binding. Thus far, the use of trivalent antimony has primarily showcased the binding of halides with few examples of polyatomic anions.²⁵ The Lewis acidity of these systems arises from polar primary bonds that result in regions of positive electrostatic potential along the extension of the bonds. Up to three of these sites can be induced. The stabilizing interaction that results from an electron

donor interacting with this site has been termed a pnictogen bond (PnB), in analogy to the closely related halogen (XB) and chalcogen (ChB) bonds $^{26-28}$ which have been employed in the design of anion receptors. $^{2,29-38}$ An important feature of these supramolecular interactions that distinguishes them from formal Lewis acids such as BX3, AlX3 or PnX5 (Pn = pnictogen, X = halogen) is that they form with minimal geometric reorganization which results in reversible PnB, ChB or XB formation without an activation barrier. 39,40 These receptors have been applied to form supramolecular capsules to mimic biological molecules, 41 as cross-membrane anion transporting agents, 4,22,36,42 and as catalysts in substitution reactions. 23,43

Figure 1. Examples of Pn(III) anion receptors. A: PnB for anion transporting and catalysis;²² B: a stibaindole system for Cl⁻ binding;¹⁹ C: PnB activation of Au–Cl bond through Cl⁻ binding.¹⁸ 1, 2, and 3: bis-Sb(III) compound for bidentate anion binding through PnBs.^{20,21}

Various anion receptors have been designed for selective solution phase binding of cyanide^{44–50} and acetate, including functionalized fluorescent calixpyrrole-typed receptors,^{51–53} urea and thiourea based receptors that are capable of selective detection of carboxylate anions,^{54–57} halogen bonding polymeric receptors that show self-healing properties,⁵⁸ and chromogenic chalcogen assisted receptors.^{59,60}

We have previously reported on the design rationale²⁰ and experimental evidence for halide binding of receptors $\mathbf{1}^{61,62}$ and $\mathbf{2}$ in both solution and the gas phase.²¹ The previously studied receptors 1 and 2 showed limited solubility in most organic solvents and intramolecular PnBs (Sb···O PnBs), which limited the anion binding affinities. Moreover, as previous solution phase studies were carried out in dimethyl sulfoxide (DMSO), the explicit binding of DMSO to the Sb(III) centers also decreased the energetics towards anion binding.²¹ Herein we report the binding properties of anion receptor 3 (Figure 1). The installation of additional tert-butyl groups was expected to minimize intermolecular aggregation, as observed in the solid state structure of 1,62 and limit intramolecular PnB formation. As a result, the solubility of 3 is greatly enhanced in non-coordinating organic solvents such as dichloromethane which, in turn, prevents competitive binding with solvents. This system is moisture-stable 61 and demonstrates high binding affinity towards pseudohalides cyanide and cyanate as well as acetate in the solution phase and can be recovered intact post-binding. The high binding affinity towards cyanide and moisture stability is tested in a phase-transfer catalyst for a Strecker cyanation reaction.

RESULTS AND DISCUSSION

Halide anion binding and origin of UV-vis absorbance changes

Previous studies revealed that compound 2 should have high binding constants to anions if competition with coordinating DMSO could be avoided.²¹ Structurally related compound 3 was prepared and found to be soluble in CH₂Cl₂. Indeed, when compound 3 was dissolved in CH2Cl2 and titrated with coordinating solvents tetrahydrofuran (THF) and DMSO, the binding constants determined by fitting the changes in the UV-vis spectra to a 1:1 (3:solvent molecule) binding model were $1.0 \times 10^2 \, M^{-1}$ and $1.2 \times 10^3 \, M^{-1}$, respectively. This corresponds to a ΔG of 17.5 kJ/mol for DMSO and supports the previous conclusions.21 Compound 3 was dissolved in CH₂Cl₂ and titrations with halide anions Cl⁻, Br⁻, and I⁻ (added as tetrabutylammonium salts, TBAX, where X = Cl-, Br-, and I-) were performed. Initial screening with chloride revealed a red-shift of the absorbance at 295 nm with increasing Cl- concentration (Figure 2). This red-shift behavior is similar to the phenomenon observed with chloride binding by telluradiazoles and tellurophenes.^{34,35} Time-dependent density functional theory (TDDFT)⁶³ calculations (S2.2 of SI) revealed that the absorption at 295 nm likely corresponds to a transition that originates in the HOMO-1 (electron density on the catecholate rings) and populates the LUMO (Sb–O σ^* orbital). A change in absorption is consistent with PnB formation at a site coincident with the LUMO. This will necessarily change the energy of the LUMO and, correspondingly, the transition.

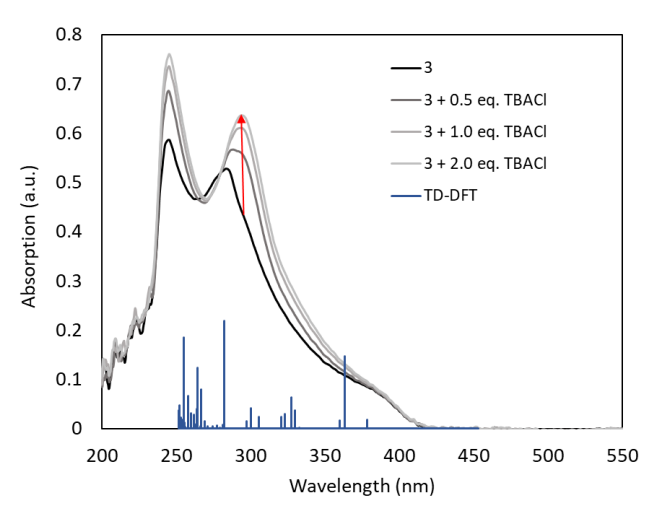


Figure 2. Representative UV-vis absorption spectra of $\bf 3$ in CH₂Cl₂ showing gradual red-shift with addition of tetrabutylammonium chloride (TBACl). Red peaks represent low-energy transitions calculated with TD-DFT.

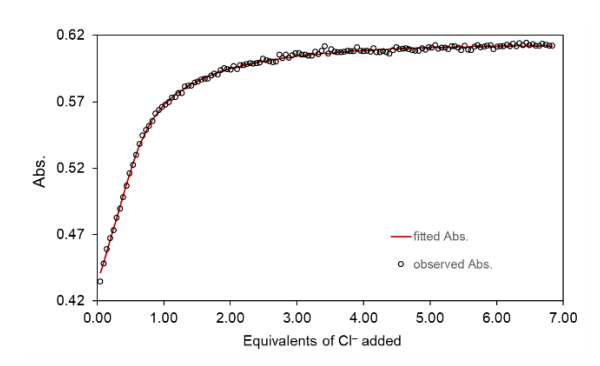
Establishment of binding models in solution phase

A simple dilution study of **3** over the concentration ranges being studied revealed the expected linear decrease in absorbance at all points, indicating that no self-aggregation of **3** can be observed in solution at these concentrations.

To quantify the solution binding of $\bf 3$ with the three halides, the change in absorption at 302 nm was extracted and different possible binding models were fit to the data to determine the most appropriate one. In all cases the ion pairing of TBA+ with X- (eq. 1) was accounted for by independently determining the dissociation constant (see S2.3 in SI) of TBAX in CD₂Cl₂ by 1 H NMR. These ion-dissociation constants (Table S4) were then explicitly included in all binding models. Step-wise equilibria (eq. 2–4) are proposed for binding of $\bf 3$ with anions:

TBAX \rightleftharpoons TBA⁺ + X⁻ (1); K₀ **3** + X⁻ \rightleftharpoons **3**·X⁻ (2); K₁₁ **3**·X⁻ + **3** \rightleftharpoons **3**₂·X⁻ (3); K₂₁ **3**·X⁻ + X⁻ \rightleftharpoons **3**·[X⁻]₂ (4); K₁₂

The data was initially fit with the simple 1:1 (of $3:X^-$) binding model described by equations 1 and 2. Analysis of the residuals revealed a non-stochastic distribution suggesting that the model did not sufficiently describe the solution behavior. More complex, stepwise-related composite models were tested against the data. The model which gave the best fit for all of the halide anions included eq. 1-3. Figure 3 illustrates the fit of this model to the chloride titration data. The experimental best-fit K_{11} from the composite model is reported in Table 1 and the results from all the models are reported in Table S5. Consistent with this model, $3:X^-$ was observed by ESI-MS. The isotopic distribution that corresponds to $3:X^-$ was only observable with higher concentrations of $3:X^-$ therefore, analysis using Job's method of continuous variation revealed a maximum that was shifted towards higher mole fractions of $3:X^-$ (Figures S36-38).



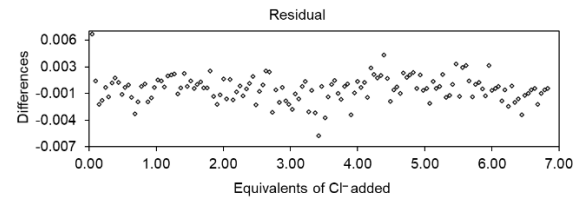


Figure 3. Fit of Cl $^-$ binding to **3** in CH $_2$ Cl $_2$ using a 2:1 and 1:1 (**3**:X $^-$) composite model.

Table 1. Summary of experimentally fitted vs. DFT calculated ΔG and K_{11} for halide anions.

	Experimental ^a		DFT ^b
	K ₁₁ (M ⁻¹)	ΔG (kJ/mol)	ΔG (kJ/mol)
CI-	8.72E+05 (0.98E+05)	-33.9 (0.3)	-19.2
Br ⁻	1.69E+04 (0.50E+04)	-24.1 (0.7)	-8.7
ŀ	2.39E+03 (1.47E+03)	-19.3 (2.4)	-2.2

^a See S2.5.9. Errors included in parentheses.

Recovery of 3 from 1:1 host:guest mixture

To verify that the observed changes correspond to host/guest complexes rather than a different reaction pathway such as substitution, experiments were performed to recover 3 from a 1:1 mixture of 3 and Cl-. Host 3 is poorly soluble in weakly coordinating solvents like CH₂Cl₂ by itself, but far more soluble when bound to an anionic guest. This experiment was used to demonstrate the reversibility of the binding. A 1:1 mixture of 3 and Cl⁻ was isolated and characterized. It was found to have ¹H NMR signatures that are distinct from the superposition of 3 and TBACI. The 1:1 mixture was dissolved in CH₂Cl₂ and treated with 1 equivalent of methyl triflate to form chloromethane and liberate the triflate anion following eq. 5. The weaker binding of triflate results in a high fraction of unbound 3 which is not very soluble and precipitates out of CH₂Cl₂ in 47% yield. The precipitate was confirmed to be 3 by ¹H NMR and EA. The remaining **3** is presumed to be soluble because of weak binding to the triflate anion according to equation 2. The triflate anion, while generally considered non-coordinating, has been observed to form a chalcogen bond with the N-methyl-2,1,3-benzotelluradiazolium cation in the solid state.⁶⁴

TBA[
$$\mathbf{3}\cdot CI$$
] + MeOTf $\rightarrow \mathbf{3}_{(s)}$ + MeCl_(g) + TBAOTf (5)

Single crystals were obtained when the previous experiment was performed by vapor diffusion of methyl triflate into a solution of TBA[3·Cl]. The quality of the data obtained from the crystal was only sufficient to determine connectivity, with a resolution of 0.86 Å, from which it was clear that host 3 was recovered intact (Figure 4). Elemental analysis (EA) of this material matched that of independently synthesized host and was consistent with the formula (see S1.2.3). These crystals revealed molecules of 3 engaging in intramolecular pnictogen bonding. This drives the head-to-tail self-assembly of the molecules into a column as depicted in Figure 4. It is presumed that the presence of this intramolecular pnictogen bonding contributes to the low solubility in non-coordinating and weakly coordinating solvents.

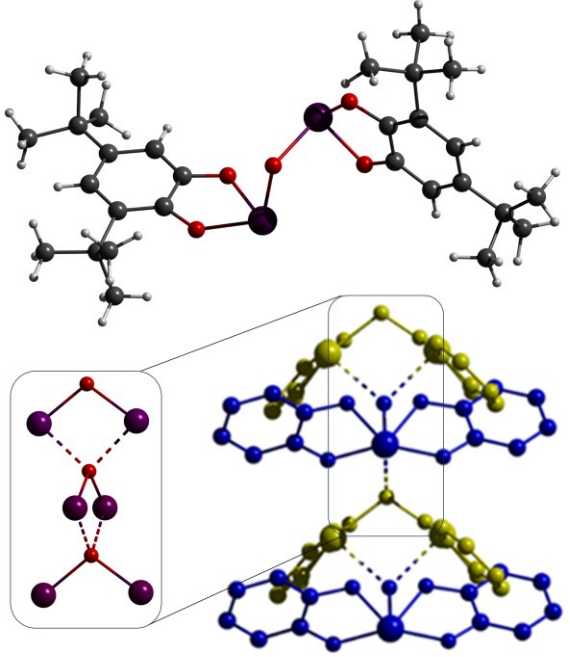


Figure 4. Ball and stick model of asymmetric unit of **3** from the single crystal structure (top); Head-to-tail assembly of **3** with PnB assignment depicted with hashed bonds. *tert*-Butyl substituents and hydrogen atoms removed for clarity (bottom right); Zoom-in of intermolecular PnBs between Sb-O-Sb bridges of **3** with catecholate removed for clarity (bottom left).

Solution binding of polyatomic anions

To take advantage of the potential bidentate motif, polyatomic anions that can bridge the two antimony centers were experimentally investigated. Tetrabutylammonium salts of CN-, OCN-, SCN-, NO₃-, and OAc- (referred to as X-) were titrated against **3**. During all titration events, an analogous red-shift was observed for the polyatomic anions consistent with binding at the sites of high V_{max} . The UV-vis titration data was extracted and fit to the same set of models as the halides involving stepwise equilibria from eq. 1-3. Very high binding affinities (with a K_{11} of over $10^7\ M^{-1}$) were observed for the basic CN- and OAc- anions. For comparison, some binding constants utilizing different bonding interactions have been listed in Tables S6-S8. Direct comparison of these results is difficult due to differences in the solvents as well as counterions that were used. Cyanide binding constants have been reported in

^b See S3.

the range of 104-108 M⁻¹.44-47,49,65,66 Acetate binding constants have been reported in the range of 10⁴-10⁶ M⁻¹.^{51,53,59,67} Cyanate binding constants have been reported in the range of 102-105 M 1.4,25,68,69 Smaller binding constants were observed between 3 and the less basic anions. Table 2 summarizes the binding constants for the 1:1 equilibria (Eq.(2)) from the best fitting model and Table S5 contains any additional equilibrium constants from the best-fitting composite models. In an attempt to rationalize the results, the free energies associated with the K₁₁ values were plotted as a function of the pK_a values for the conjugate acids of the anions in H₂O, DMSO, acetonitrile (ACN) and dichloroethane (DCE).⁷⁰ In all cases where pKa's had been determined, the correlation was high (0.97-0.98) except for aqueous pK_a's (Figure S42). The strong correlation supports the accuracy of the models used for fitting and lends credence to the fact that no change could be observed upon addition of a PF₆⁻ source.

Table 2. Summary of experimentally fitted vs. DFT calculated ΔG and K_{11} for polyatomic anions.

	Experimental ^a		DFT ^b
	K ₁₁ (M ⁻¹)	ΔG (kJ/mol)	ΔG (kJ/mol)
OAc-	2.82E+08 (1.02E+08)	-48.8 (1.0)	-38.4
CN-	1.69E+08 (0.97E+08)	-46.0 (1.4)	-31.6
OCN-	9.54E+07 (6.20E+07)	-45.5 (1.8)	-29.2
NO ₃ -	1.59E+04 (0.26E+04)	-24.0 (0.4)	-7.74
SCN-	3.20E+03 (1.64E+03)	-20.9 (3.2)	-6.1

 $^{^{\}it a}$ See S2.5.9. Errors included in parentheses.

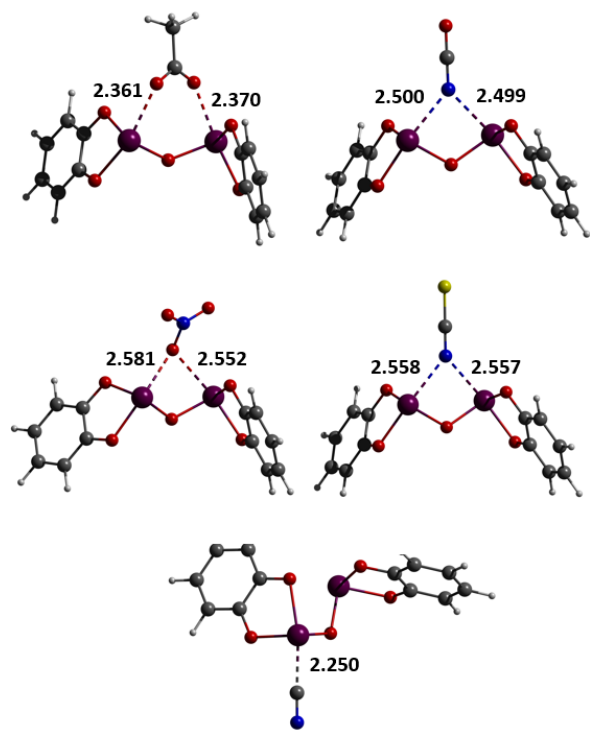


Figure 5. DFT calculated structures of polyatomic complexes 3·X⁻.

DFT calculations were performed on the 1:1 complexes with all of the anions to gain some insight into the structures and to corroborate the measured binding constants. The B97-D3 functional, which accounts for dispersion,71 along with the conductor-like polarizable continuum model (CPCM)72 to account for implicit solvation were used. This method has previously been demonstrated to accurately reproduce the trends in the free energy of anion binding using chalcogen bonding.³⁴ As the *tert*-butyl groups are not expected to affect the final binding energetics, compound 1 was used as a computationally more simple model for 3 in all binding calculations. All structures were optimized from a variety of starting geometries that include a bridging anion, a terminal anion and, in the cases of the pseudohalogens, binding from either N or C/O/S. Structures containing Cl⁻, Br⁻ and CN⁻ (κ-C) were predicted to adopt a monodentate geometry. In contrast, the larger anions are all predicted to adopted conformations with bridging anions as the global minima (Figure 5 and S98). A local minimum for terminal binding was found within 3 kJ/mol in all cases except for OAc-. The cyanate and thiocyanate anions were both predicted to be bound through the nitrogen atom rather than the chalcogen. The tight binding to cyanide is consistent with the short Sb···CNdistance (2.25 Å) which is only 0.05 Å longer than the average Sb-C covalent bond distance.73 The acetate anion is predicted to bridge the two antimony centers with short Sb···O PnBs. DFT predictions of the free energy for the formation of the 1:1 complex (3·X⁻) in solution revealed energies (Table 2) that are, on average, 18 kJ/mol higher in energy than the experimental values. This is reproduced in the linear regression and is an offset error that likely results from incorrect assumptions about the equivalency of 1 and 3. The strong linear correlation (Figure 6) between experiments and calculations gives confidence in the model that was used and further confirms the utility of DFT for predicting trends (rather

^b See S3.

than absolute values). The deviation of the slope from unity suggests that there is some refinement that can be made to the computational method, although it is not clear if it is the basis set, functional, relativistic correction or the solvation model (or a combination of these) that is responsible for the deviation.

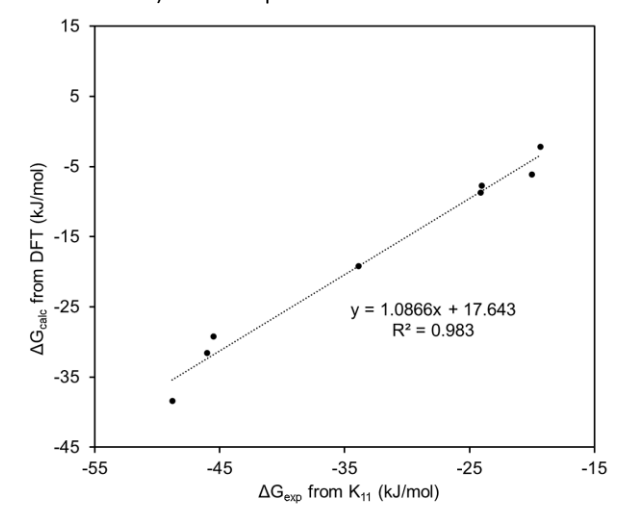


Figure 6. DFT calculated ΔG values for the 1:1 complexes ($\mathbf{3} \cdot X^-$) vs experimental values derived from the K_{11} binding constants. Results of linear regression provided for all anions.

Qualitative NMR experiments and ESI-MS measurements

The excellent fit between the equilibrium models and the titration data, along with the strong correlation between experimental K₁₁ values and pKa's and DFT calculated ΔG values is strong evidence that the general model for anion binding is correct. Without structural data, however, further evidence of the accuracy of this model was desired. Solution titrations were performed in CD₂Cl₂, where 3 was treated with 0-5 equiv. of TBAX and monitored by 1H NMR (see Figure 7 and section S2.8 in SI). The results are qualitative as 3 is not completely soluble in CD₂Cl₂ at concentrations relevant for NMR studies. Complete dissolution is observed upon addition of 1-2 equivalents of TBAX in all cases. For the more weakly binding $X^- = I^-$, SCN⁻ and NO_3^- a shift in the aromatic resonances associated with the aromatic hydrogen atoms on the catecholate rings of 3 is observed as the concentration of TBAX is increased (Figure 7, top). This is consistent with two species in dynamic equilibrium under fast exchange and these are assigned as 3 and 3·X⁻. These assignments are consistent with the ¹H NMR titration results for TBAI with 2 previously reported in DMSO.²¹ For the tighter binding anions (X⁻ = Cl⁻, Br⁻, OCN⁻, OAc⁻ and CN⁻) the changes observed by ¹H NMR are consistent with those observed in the previous report when 2 is titrated with TBABr or TBACl in DMSO.²¹ The set of resonances associated with the aromatic hydrogen atoms in unbound 3 shift to lower frequency with the addition of anion. At a certain point, a new set of resonances grows in at a lower frequency. The first shift corresponds to two species in dynamic equilibrium under fast exchange (assigned to 3 and 3₂·X⁻), while the new resonances that grow in correspond to a species in the slow exchange regime (assigned to 3·X-). This assignment agrees with the previous study,²¹ and is consistent with higher concentrations of 32·X- at lower concentrations of TBAX and higher concentrations of 3·X⁻ at higher concentrations of TBAX.

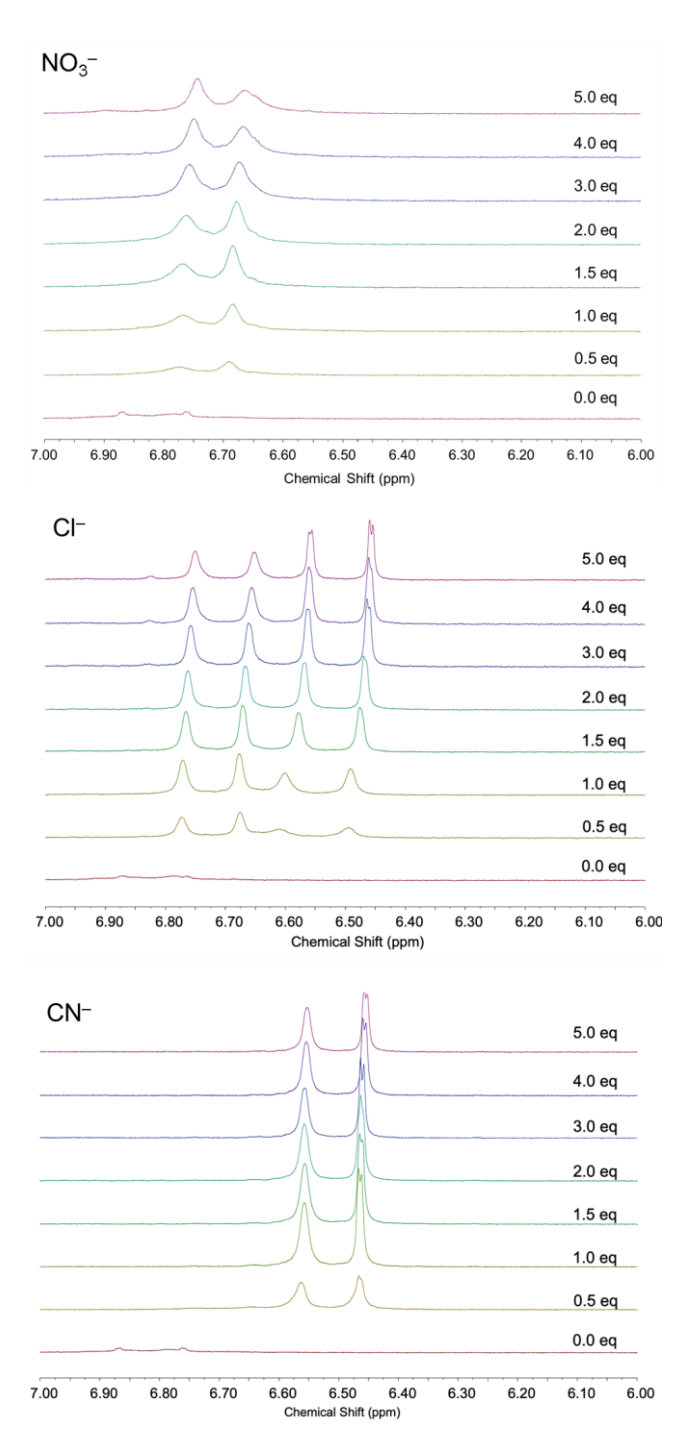


Figure 7. Stacked ¹H NMR spectrum of aromatic region of **3** with varying equivalents of anion.

In the cases of the tightest binding anions, CN⁻ and OAc⁻, an additional experiment was performed to confirm the reversibility of the anion binding, and thereby demonstrate that a decomposition process is not responsible for the observed changes. The same process for recovering **3** from TBA[**3**·Cl] was performed and yielded similar results (47% yield with TBAOAc and 45% yield with TBACN). Depending on rate of crystallization, two solids with slightly different IR spectra were obtained from the 1:1 mixture of

3 and TBAOAc (see S2.9.2). This is attributed to polymorphism. The ¹H NMR spectrum of both solids confirmed that they were identical products (see S2.9.1). On fast addition of MeOTf, the FTIR spectrum directly matched that of **3** that had been recovered from the 1:1 mixture of TBA[**3**·Cl] (the identity was confirmed by EA and single crystal structural determination, vide supra). With vapor diffusion of MeOTf, the FTIR spectrum precisely matched that of the as-synthesized **3** (the identity was confirmed by EA and single crystal data of the pyridine solvate).²⁰

Corroborating evidence for the stoichiometries of the species in solution was obtained using negative-mode ESI-MS (see SI section S1.10 and S2.10). Solutions of 3 with 0.5 or one equivalent of TBAX were prepared in CH₂Cl₂ and, after filtration, diluted with methanol. Injection of these samples directly into the spectrometer revealed isotopic distributions associated with 3·X⁻ in all cases except when $X^- = CN^-$. An isotopic distribution corresponding to $3_2 \cdot X^$ was observed in all cases except when X⁻ = OAc⁻, OCN⁻ or CN⁻. This provides strong evidence that these species are present in solution. In all cases, two isotopic distributions were observed (413 and 561 m/z) that were independent of the anion that was used. These are presumed to be the result of fragmentation due to the formation of chloride and organic radicals from the reduction of the CH₂Cl₂ under the high negative voltage of the electrospray capillary.74,75 This is supported by the efficient bulk recovery of 3 from CH_2Cl_2 solutions of TBA[3·X] (X = Cl, CN and OAc) as detailed above.

The combined evidence from the UV-vis titrations, ¹H NMR titrations, competition experiments, recovery experiments, and ESI-MS provide strong support for the binding of **3** to the anions according to the proposed models.

Catalysis with CN⁻ binding

+ CN:
$$\frac{H_2O}{CH_2Cl_2}$$
 HN CN

Scheme 1. Strecker reaction of aldimine with phase-transfer catalysis. 76

As the observed binding energy with CN⁻ was within the range associated with selective CN $^{\!-}$ receptors $^{\!44-47,77}$ and $\boldsymbol{3}$ was found to be moisture stable (see Figure S2.1), 3 appeared to be a good candidate to test as a noncovalent catalyst using a cyanation reaction.⁷⁸ To demonstrate the moisture stability of 3, a Strecker cyanation of an aldimine under phase-transfer conditions (CH₂Cl₂ and water)⁷⁶ was performed (Scheme 1) where 3 was anticipated to accelerate the reaction by aiding in the transfer of the CN⁻ anion from the aqueous phase into the organic phase. A doubling of the initial rate of formation of the product (5) beyond the uncatalyzed reaction was observed in the presence of 3 (0.7 mol% catalyst loading) based on the yield of product measured at 5 min. A final yield that was approximately 40% higher in the presence of the catalyst was also observed (Figure S97). Control reactions with SbCl₃ or Ph₃Sb showed very little formation of the desired nitrile product, suggesting an inhibition of the reaction which stands in stark contrast to the performance of 3. Control reactions with catechol only or

catechol and $SbCl_3$ gave no enhancement over the uncatalyzed trials, indicating that the anticipated hydrolysis products were not responsible for catalyzing the reaction.

CONCLUSION

In conclusion, the binding of receptor $\bf 3$ to various anions has been studied in CH_2Cl_2 solution by taking advantage of the observed changes to the absorption spectrum. Very high binding constants were observed with basic anions CN^- , OCN^- and OAc^- . The binding constants were well-reproduced by DFT models that included solvation. The binding models were further corroborated by NMR, host recovery experiments, and ESI-MS measurements. It was demonstrated that water-stable $\bf 3$ can catalyze the Strecker cyanation of an aldimine under phase-transfer conditions. These studies should encourage the continued application of pnictogen bonding, harnessing the wealth of established trivalent antimony chemistry, in the design of anion receptors and noncovalent catalysts.

ASSOCIATED CONTENT

Supporting Information

Experimental details including titration and fitting methodologies, catalysis experiments, DFT calculations, ¹H NMR, ESI- MS. DFT optimized coordinates are provided as .xyz files. R scripts are provided for all models studied here. The electronic supporting information is available free of charge via the internet at http://pubs.acs.org.

Accession Codes

CCDC 2256517 contains the supplementary crystallographic data for this paper. This data can be obtained free of charge via www.ccdc.cam.ac.uk/data_request/cif, or by emailing data_request@ccdc.cam.ac.uk, or by contacting The Cambridge Crystallographic Data Centre, 12 Union Road, Cambridge CB2 1EZ, UK; fax: +44 1223 336033

AUTHOR INFORMATION

Corresponding Author

Anthony F. Cozzolino. Email: anthony.f.Cozzolino@ttu.edu.

AUTHOR CONTRIBUTIONS

AFC, JQ, and CNB were responsible for conceptualization, synthesis and experimental work. SL and XL performed and analyzed MS experiments. GCG, JDG and SV collected/analyzed the crystallographic data. All authors were involved in writing and editing the manuscript.

ACKNOWLEDGMENT

Research funding (CHE 1847878) and instrument support (NMR: CHE 1048553) from the National Science Foundation are gratefully acknowledged.

REFERENCES

- (1) Custelcean, R. Anions in Crystal Engineering. *Chem. Soc. Rev.* **2010**, *39* (10), 3675. https://doi.org/10.1039/b926221k.
- (2) Tresca, B. W.; Berryman, O. B.; Zakharov, L. N.; Johnson, D. W.; Haley, M. M. Anion-Directed Self-Assembly of a 2,6-Bis(2-Anilinoethynyl)Pyridine Bis(Amide) Scaffold. *Supramol. Chem.* **2016**, *28* (1–2), 37–44. https://doi.org/10.1080/10610278.2015.1072199.
- (3) Gale, P. A.; Caltagirone, C. Anion Sensing by Small Molecules and Molecular Ensembles. *Chem Soc Rev* **2015**, *44* (13), 4212–4227. https://doi.org/10.1039/C4CS00179F.
- (4) Docker, A.; Marques, I.; Kuhn, H.; Zhang, Z.; Félix, V.; Beer, P. D. Selective Potassium Chloride Recognition, Sensing, Extraction, and Transport Using a Chalcogen-Bonding Heteroditopic Receptor. *J. Am. Chem. Soc.* **2022**, *144* (32), 14778–14789. https://doi.org/10.1021/jacs.2c05333.
- (5) Gale, P. A.; Howe, E. N. W.; Wu, X. Anion Receptor Chemistry. *Chem* **2016**, *1* (3), 351–422. https://doi.org/10.1016/j.chempr.2016.08.004.
- (6) Lim, J. Y. C.; Beer, P. D. Sigma-Hole Interactions in Anion Recognition. *Chem* **2018**, *4* (4), 731–783. https://doi.org/10.1016/j.chempr.2018.02.022.
- (7) Christianson, A. M.; Rivard, E.; Gabbaï, F. P. $1\lambda5$ -Stibaindoles as Lewis Acidic, π -Conjugated, Fluoride Anion Responsive Platforms. *Organometallics* **2017**, *36* (14), 2670–2676. https://doi.org/10.1021/acs.organomet.7b00289.
- (8) Christianson, A. M.; Gabbaï, F. P. Anion Sensing with a Lewis Acidic BODIPY-Antimony(V) Derivative. *Chem. Commun.* **2017**, *53* (16), 2471–2474. https://doi.org/10.1039/C6CC09205E.
- (9) Yang, M.; Tofan, D.; Chen, C.-H.; Jack, K. M.; Gabbaï, F. P. Digging the Sigma-Hole of Organoantimony Lewis Acids by Oxidation. *Angew. Chem. Int. Ed.* **2018**, *57* (42), 13868–13872. https://doi.org/10.1002/anie.201808551.
- (10) Chen, C.-H.; Gabbaï, F. P. Fluoride Anion Complexation by a Triptycene-Based Distiborane: Taking Advantage of a Weak but Observable C-H···F Interaction. *Angew. Chem. Int. Ed.* **2017**, *56* (7), 1799–1804. https://doi.org/10.1002/anie.201611009.
- (11) Kumar, A.; Yang, M.; Kim, M.; Gabbaï, F. P.; Lee, M. H. OFF–ON Fluorescence Sensing of Fluoride by Donor–Antimony(V) Lewis Acids. *Organometallics* **2017**, *36* (24), 4901–4907. https://doi.org/10.1021/acs.organomet.7b00759.
- (12) Hirai, M.; Gabbaï, F. P. Squeezing Fluoride out of Water with a Neutral Bidentate Antimony(V) Lewis Acid. *Angew. Chem. Int. Ed.* **2015**, *54* (4), 1205–1209. https://doi.org/10.1002/anie.201410085.
- (13) Smith, J. E.; Gabbaï, F. P. Are Ar3SbCl2 Species Lewis Acidic? Exploration of the Concept and Pnictogen Bond Catalysis Using a Geometrically Constrained Example. *Organometallics* **2023**, *42* (3), 240–245. https://doi.org/10.1021/acs.organomet.2c00565.
- (14) Jones, J. S.; Gabbaï, F. P. Coordination- and Redox-Noninnocent Behavior of Ambiphilic Ligands Containing Antimony. *Acc. Chem. Res.* **2016**, *49* (5), 857–867. https://doi.org/10.1021/acs.accounts.5b00543.
- (15) Taylor, W. V.; Xie, Z.-L.; Cool, N. I.; Shubert, S. A.; Rose, M. J. Syntheses, Structures, and Characterization of Nickel(II) Stibines: Steric and Electronic Rationale for Metal Deposition. *Inorg. Chem.* **2018**, *57* (16), 10364–10374. https://doi.org/10.1021/acs.inorgchem.8b01565.
- (16) Taylor, W. V.; Cammack, C. X.; Shubert, S. A.; Rose, M. J. Thermoluminescent Antimony-Supported Copper-Iodo Cuboids: Approaching NIR Emission via High Crystallographic Symmetry. *Inorg. Chem.* **2019**. https://doi.org/10.1021/acs.inorgchem.9b00229.
- (17) Jiménez-Tenorio, M.; Puerta, M. C.; Salcedo, I.; Valerga, P.; Ríos, I. de los; Mereiter, K. Oligomerization of Styrenes Mediated by Cationic Allyl Nickel Complexes Containing Triphenylstibine or Triphenylarsine. *Dalton Trans.* **2009**, No. 10, 1842–1852. https://doi.org/10.1039/B818784C.
- (18) Jones, J. S.; Gabbaï, F. P. Activation of an Au–Cl Bond by a Pendent SbIII Lewis Acid: Impact on Structure and Catalytic Activity. *Chem. Eur. J.* **2017**, 23 (5), 1136–1144. https://doi.org/10.1002/chem.201604521.

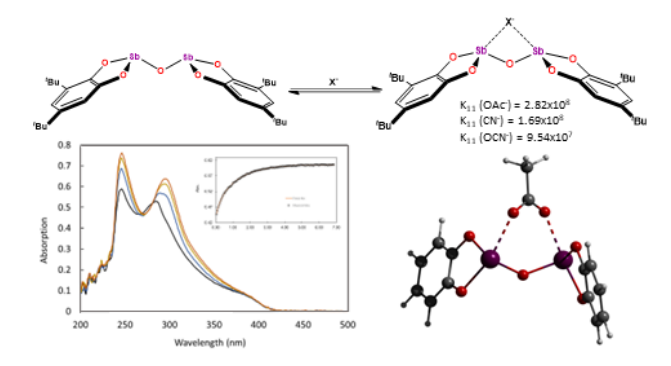
- (19) Christianson, A. M.; Gabbaï, F. P. A Lewis Acidic, π -Conjugated Stibaindole with a Colorimetric Response to Anion Binding at Sb(III). *Organometallics* **2017**, *36* (16), 3013–3015. https://doi.org/10.1021/acs.organomet.7b00419.
- (20) Qiu, J.; Unruh, D. K.; Cozzolino, A. F. The Design, Synthesis and Structural Characterization of a Bis-Antimony(III) Compound for Anion Binding and the DFT Evaluation of Halide Binding through Antimony Secondary Bonding Interactions. *J. Phys. Chem. A* **2016**, *120* (46), 9257–9269. https://doi.org/10.1021/acs.jpca.6b08170.
- (21) Qiu, J.; Song, B.; Li, X.; Cozzolino, A. F. Solution and Gas Phase Evidence of Anion Binding through the Secondary Bonding Interactions of a Bidentate Bis-Antimony(III) Anion Receptor. *Phys. Chem. Chem. Phys.* **2018**, *20* (1), 46–50. https://doi.org/10.1039/C7CP05933G.
- (22) Lee, L. M.; Tsemperouli, M.; Poblador-Bahamonde, A. I.; Benz, S.; Sakai, N.; Sugihara, K.; Matile, S. Anion Transport with Pnictogen Bonds in Direct Comparison with Chalcogen and Halogen Bonds. *J. Am. Chem. Soc.* **2019**, *141* (2), 810–814. https://doi.org/10.1021/jacs.8b12554.
- (23) Benz Sebastian; Poblador-Bahamonde Amalia I.; Low-Ders Nicolas; Matile Stefan. Catalysis with Pnictogen, Chalcogen, and Halogen Bonds. *Angew. Chem. Int. Ed.* **2018**, *0* (0). https://doi.org/10.1002/anie.201801452.
- (24) Marczenko, K. M.; Jee, S.; Chitnis, S. S. High Lewis Acidity at Planar, Trivalent, and Neutral Bismuth Centers. *Organometallics* **2020**, *39* (23), 4287–4296. https://doi.org/10.1021/acs.organomet.0c00378.
- (25) Kuhn, H.; Docker, A.; Beer, P. D. Anion Recognition with Antimony(III) and Bismuth(III) Triaryl-Based Pnictogen Bonding Receptors. *Chem. Eur. J.* **2022**, *28* (67), e202201838. https://doi.org/10.1002/chem.202201838.
- (26) Metrangolo, P.; Resnati, G. Halogen Bonding: A Paradigm in Supramolecular Chemistry. *Chem. Eur. J.* **2001**, *7* (12), 2511–2519.
- (27) Desiraju, G. R.; Ho, P. S.; Kloo, L.; Legon, A. C.; Marquardt, R.; Metrangolo, P.; Politzer, P.; Resnati, G.; Rissanen, K. Definition of the Halogen Bond (IUPAC Recommendations 2013). *Pure Appl. Chem.* **2013**, *85* (8), 1711–1713. https://doi.org/10.1351/PAC-REC-12-05-10.
- (28) Cavallo, G.; Metrangolo, P.; Pilati, T.; Resnati, G.; Terraneo, G. Naming Interactions from the Electrophilic Site. *Cryst. Growth Des.* **2014**, *14* (6), 2697–2702. https://doi.org/10.1021/cg5001717.
- (29) Dimitrijević, E.; Kvak, O.; Taylor, M. S. Measurements of Weak Halogen Bond Donor Abilities with Tridentate Anion Receptors. *Chem. Commun.* **2010**, *46* (47), 9025–9027. https://doi.org/10.1039/COCC03347B.
- (30) Lohrman, J. A.; Deng, C.-L.; Shear, T. A.; Zakharov, L. N.; Haley, M. M.; Johnson, D. W. Methanesulfonyl-Polarized Halogen Bonding Enables Strong Halide Recognition in an Arylethynyl Anion Receptor. *Chem. Commun.* **2019**, 55 (13), 1919–1922. https://doi.org/10.1039/C8CC09251F.
- (31) Mullaney, B. R.; Partridge, B. E.; Beer, P. D. A Halogen-Bonding Bis-Triazolium Rotaxane for Halide-Selective Anion Recognition. *Chem. Eur. J.* **2015**, *21* (4), 1660–1665. https://doi.org/10.1002/chem.201405578.
- (32) Taylor, M. S. Anion Recognition in Solution via Halogen Bonding. In *Halogen Bonding II: Impact on Materials Chemistry and Life Sciences*; Metrangolo, P., Resnati, G., Eds.; Topics in Current Chemistry; Springer International Publishing: Cham, 2015; pp 27–48. https://doi.org/10.1007/128_2014_588.
- (33) Metrangolo, P.; Pilati, T.; Terraneo, G.; Biella, S.; Resnati, G. Anion Coordination and Anion-Templated Assembly under Halogen Bonding Control. *CrystEngComm* **2009**, *11* (7), 1187–1187. https://doi.org/10.1039/b821300c.
- (34) Garrett, G. E.; Gibson, G. L.; Straus, R. N.; Seferos, D. S.; Taylor, M. S. Chalcogen Bonding in Solution: Interactions of Benzotelluradiazoles with Anionic and Uncharged Lewis Bases. *J. Am. Chem. Soc.* **2015**, *137* (12), 4126–4133. https://doi.org/10.1021/ja512183e.

- (35) E. Garrett, G.; I. Carrera, E.; S. Seferos, D.; S. Taylor, M. Anion Recognition by a Bidentate Chalcogen Bond Donor. *Chem. Commun.* **2016**, *52* (64), 9881–9884. https://doi.org/10.1039/C6CC04818H.
- (36) Benz, S.; Macchione, M.; Verolet, Q.; Mareda, J.; Sakai, N.; Matile, S. Anion Transport with Chalcogen Bonds. *J. Am. Chem. Soc.* **2016**, *138* (29), 9093–9096. https://doi.org/10.1021/jacs.6b05779.
- (37) Docker, A.; Johnson, T. G.; Kuhn, H.; Zhang, Z.; Langton, M. J. Multistate Redox-Switchable Ion Transport Using Chalcogen-Bonding Anionophores. *J. Am. Chem. Soc.* **2023**, *145* (4), 2661–2668. https://doi.org/10.1021/jacs.2c12892.
- (38) Hein, R.; Docker, A.; Davis, J. J.; Beer, P. D. Redox-Switchable Chalcogen Bonding for Anion Recognition and Sensing. *J. Am. Chem. Soc.* **2022**, *144* (19), 8827–8836. https://doi.org/10.1021/jacs.2c02924.
- (39) Cozzolino, A. F.; Vargas-Baca, I.; Mansour, S.; Mahmoudkhani, A. H. The Nature of the Supramolecular Association of 1,2,5-Chalcogenadiazoles. *J. Am. Chem. Soc.* **2005**, *127* (9), 3184–3190. https://doi.org/10.1021/ja044005y.
- (40) Riley, K. E.; Hobza, P. The Relative Roles of Electrostatics and Dispersion in the Stabilization of Halogen Bonds. *Phys. Chem. Chem. Phys.* **2013**, *15* (41), 17742–17751. https://doi.org/10.1039/C3CP52768A.
- (41) Riwar, L.-J.; Trapp, N.; Root, K.; Zenobi, R.; Diederich, F. Supramolecular Capsules: Strong versus Weak Chalcogen Bonding. *Angew. Chem. Int. Ed.* **2018**, 57 (52), 17259–17264. https://doi.org/10.1002/anie.201812095.
- (42) Park, G.; Brock, D. J.; Pellois, J.-P.; Gabbaï, F. P. Heavy Pnictogenium Cations as Transmembrane Anion Transporters in Vesicles and Erythrocytes. *Chem* **2019**, 5 (8), 2215–2227. https://doi.org/10.1016/j.chempr.2019.06.013.
- (43) Benz, S.; Mareda, J.; Besnard, C.; Sakai, N.; Matile, S. Catalysis with Chalcogen Bonds: Neutral Benzodiselenazole Scaffolds with High-Precision Selenium Donors of Variable Strength. *Chem. Sci.* **2017**, *8* (12), 8164–8169. https://doi.org/10.1039/C7SC03866F.
- (44) Hudnall, T. W.; Gabbaï, F. P. Ammonium Boranes for the Selective Complexation of Cyanide or Fluoride Ions in Water. *J. Am. Chem. Soc.* **2007**, *129* (39), 11978–11986. https://doi.org/10.1021/ja073793z.
- (45) Wade, C. R.; Gabbaï, F. P. Cyanide Anion Binding by a Triarylborane at the Outer Rim of a Cyclometalated Ruthenium(II) Cationic Complex. *Inorg. Chem.* **2010**, *49* (2), 714–720. https://doi.org/10.1021/ic9020349.
- (46) Kim, Y.; Huh, H.-S.; Lee, M. H.; Lenov, I. L.; Zhao, H.; Gabbaï, F. P. Turn-On Fluorescence Sensing of Cyanide Ions in Aqueous Solution at Parts-per-Billion Concentrations. *Chem. Eur. J.* **2011**, *17* (7), 2057–2062. https://doi.org/10.1002/chem.201002861.
- (47) Song, K. C.; Lee, K. M.; Nghia, N. V.; Sung, W. Y.; Do, Y.; Lee, M. H. Synthesis and Anion Binding Properties of Multi-Phosphonium Triarylboranes: Selective Sensing of Cyanide Ions in Buffered Water at PH 7. *Organometallics* **2013**, 32 (3), 817–823. https://doi.org/10.1021/om3010542.
- (48) Chen, C.-H.; P. Gabbaï, F. Large-Bite Diboranes for the $\mu(1,2)$ Complexation of Hydrazine and Cyanide. *Chem. Sci.* **2018**, *9* (29), 6210–6218. https://doi.org/10.1039/C8SC01877D.
- (49) Christianson, A. M.; Gabbaï, F. P. Fluoride and Cyanide Anion Sensing by an Sb(V)-Substituted Cyclometalated Ru Polypyridyl Complex. *J. Organomet. Chem.* **2017**, *847*, 154–161. https://doi.org/10.1016/j.jorganchem.2017.03.012.
- (50) Wade, C. R.; Gabbaï, F. P. Cyanide and Azide Anion Complexation by a Bidentate Stibonium-Borane Lewis Acid. *Z. Für Naturforschung B* **2015**, *69* (11–12), 1199–1205. https://doi.org/10.5560/znb.2014-4168.
- (51) Anzenbacher, P.; Liu, Y.; Palacios, M. A.; Minami, T.; Wang, Z.; Nishiyabu, R. Leveraging Material Properties in Fluorescence Anion Sensor Arrays: A General Approach. *Chem. Eur. J.* **2013**, *19* (26), 8497–8506. https://doi.org/10.1002/chem.201204188.
- (52) Pushina, M.; Koutnik, P.; Nishiyabu, R.; Minami, T.; Savechenkov, P.; Anzenbacher, P. Anion Sensing by Fluorescent Expanded

- Calixpyrroles. *Chem. Eur. J.* **2018**, *24* (19), 4879–4884. https://doi.org/10.1002/chem.201705387.
- (53) Liu, Y.; Minami, T.; Nishiyabu, R.; Wang, Z.; Anzenbacher, P. Sensing of Carboxylate Drugs in Urine by a Supramolecular Sensor Array. *J. Am. Chem. Soc.* **2013**, *135* (20), 7705–7712. https://doi.org/10.1021/ja4015748.
- (54) Lichosyt, D.; Wasiłek, S.; Jurczak, J. Exploring the Chiral Recognition of Carboxylates by C2-Symmetric Receptors Bearing Glucosamine Pendant Arms. *J. Org. Chem.* **2016**, *81* (17), 7342–7348. https://doi.org/10.1021/acs.joc.6b00763.
- (55) Cholewiak, A.; Tycz, A.; Jurczak, J. 8-Propyldithieno[3,2-b:2',3'-e]Pyridine-3,5-Diamine (DITIPIRAM) Derivatives as Neutral Receptors Tailored for Binding of Carboxylates. *Org. Lett.* **2017**, *19* (11), 3001–3004. https://doi.org/10.1021/acs.orglett.7b01235.
- (56) Piątek, P. A Selective Chromogenic Chemosensor for Carboxylate Salt Recognition. *Chem. Commun.* **2011**, *47* (16), 4745–4747. https://doi.org/10.1039/COCC05537A.
- (57) He, X.; Herranz, F.; Cheng, E. C.-C.; Vilar, R.; Yam, V. W.-W. Design, Synthesis, Photophysics, and Anion-Binding Studies of Bis(Dicyclohexylphosphino)Methane-Containing Dinuclear Gold(I) Thiolate Complexes with Urea Receptors. *Chem. Eur. J.* **2010**, *16* (30), 9123–9131. https://doi.org/10.1002/chem.201000647.
- (58) Tepper, R.; Bode, S.; Geitner, R.; Jäger, M.; Görls, H.; Vitz, J.; Dietzek, B.; Schmitt, M.; Popp, J.; Hager, M. D.; Schubert, U. S. Polymeric Halogen-Bond-Based Donor Systems Showing Self-Healing Behavior in Thin Films. *Angew. Chem. Int. Ed.* **2017**, *56* (14), 4047–4051. https://doi.org/10.1002/anie.201610406.
- (59) Goswami, S.; Hazra, A.; Chakrabarty, R.; Fun, H.-K. Recognition of Carboxylate Anions and Carboxylic Acids by Selenium-Based New Chromogenic Fluorescent Sensor: A Remarkable Fluorescence Enhancement of Hindered Carboxylates. *Org. Lett.* **2009**, *11* (19), 4350–4353. https://doi.org/10.1021/ol901737s.
- (60) Goswami, S.; Hazra, A.; Das, M. K. Selenodiazole-Fused Diacetamidopyrimidine, a Selective Fluorescence Sensor for Aliphatic Monocarboxylates. *Tetrahedron Lett.* **2010**, *51* (25), 3320–3323. https://doi.org/10.1016/j.tetlet.2010.04.085.
- (61) Anchisi, C.; Corda, L.; Maccioni, A.; Podda, G.; Cabiddu, S. Studies on the Synthesis of Heterocyclic Compounds. Synthesis of 1,3,2-Benzoxathia- and 1,3,2-Benzodioxastibole Derivatives. *J. Heterocycl. Chem.* **1976**, *13* (5), 1033–1036. https://doi.org/10.1002/jhet.5570130519.
- (62) Biros, S. M.; Bridgewater, B. M.; Villeges-Estrada, A.; Tanski, J. M.; Parkin, G. Antimony Ethylene Glycolate and Catecholate Compounds: Structural Characterization of Polyesterification Catalysts. *Inorg. Chem.* **2002**, *41* (15), 4051–4057. https://doi.org/10.1021/ic020204b.
- (63) Petrenko, T.; Kossmann, S.; Neese, F. Efficient Time-Dependent Density Functional Theory Approximations for Hybrid Density Functionals: Analytical Gradients and Parallelization. *J. Chem. Phys.* **2011**, *134* (5), 054116. https://doi.org/10.1063/1.3533441.
- (64) Risto, M.; Reed, R. W.; Robertson, C. M.; Oilunkaniemi, R.; Laitinen, R. S.; Oakley, R. T. Self-Association of the N-Methyl Benzotelluro-diazolylium Cation: Implications for the Generation of Super-Heavy Atom Radicals. *Chem. Commun.* **2008**, No. 28, 3278–3280. https://doi.org/10.1039/b803159b.
- (65) Broomsgrove, A. E. J.; A. Addy, D.; Di Paolo, A.; Morgan, I. R.; Bresner, C.; Chislett, V.; Fallis, I. A.; Thompson, A. L.; Vidovic, D.; Aldridge, S. Evaluation of Electronics, Electrostatics and Hydrogen Bond Cooperativity in the Binding of Cyanide and Fluoride by Lewis Acidic Ferrocenylboranes. *Inorg. Chem.* **2010**, *49* (1), 157–173. https://doi.org/10.1021/ic901673u.
- (66) Huh, J. O.; Do, Y.; Lee, M. H. A BODIPY–Borane Dyad for the Selective Complexation of Cyanide Ion. *Organometallics* **2008**, *27* (6), 1022–1025. https://doi.org/10.1021/om701237t.
- (67) Akdeniz, A.; Minami, T.; Watanabe, S.; Yokoyama, M.; Ema, T.; Anzenbacher, P. Determination of Enantiomeric Excess of Carboxylates by

- Fluorescent Macrocyclic Sensors. *Chem. Sci.* **2016**, *7* (3), 2016–2022. https://doi.org/10.1039/C5SC04235F.
- (68) Bozkurt, S.; Halay, E.; Durmaz, M.; Topkafa, M.; Ceylan, Ö. A Novel Turn-on Fluorometric "Reporter-Spacer-Receptor" Chemosensor Based on Calix[4]Arene Scaffold for Detection of Cyanate Anion. *J. Heterocycl. Chem.* **2021**, *58* (5), 1079–1088. https://doi.org/10.1002/jhet.4238.
- (69) V. Rosokha, S.; L. Stern, C.; Swartz, A.; Stewart, R. Halogen Bonding of Electrophilic Bromocarbons with Pseudohalide Anions. *Phys. Chem. Chem. Phys.* **2014**, *16* (25), 12968–12979. https://doi.org/10.1039/C4CP00976B.
- (70) Kütt, A.; Selberg, S.; Kaljurand, I.; Tshepelevitsh, S.; Heering, A.; Darnell, A.; Kaupmees, K.; Piirsalu, M.; Leito, I. PKa Values in Organic Chemistry Making Maximum Use of the Available Data. *Tetrahedron Lett.* **2018**, *59* (42), 3738–3748. https://doi.org/10.1016/j.tetlet.2018.08.054.
- (71) Semiempirical GGA-type density functional constructed with a long-range dispersion correction Grimme 2006 Journal of Computational Chemistry Wiley Online Library. https://onlinelibrary.wiley.com/doi/full/10.1002/jcc.20495 (accessed 2019-06-10).
- (72) Grimme, S.; Ehrlich, S.; Goerigk, L. Effect of the Damping Function in Dispersion Corrected Density Functional Theory. *J. Comput. Chem.* **2011**, *32* (7), 1456–1465. https://doi.org/10.1002/jcc.21759.
- (73) Weast, R. C.; Astle, M. J. CRC Handbook of Chemistry and Physics, 63rd ed.; CRC Press, 1982.
- (74) Zhu, J.; Cole, R. B. Formation and Decompositions of Chloride Adduct Ions, [M + Cl]–, in Negative Ion Electrospray Ionization Mass Spectrometry. *J. Am. Soc. Mass Spectrom.* **2000**, *11* (11), 932–941. https://doi.org/10.1016/S1044-0305(00)00164-1.
- (75) Cole, R. B.; Harrata, A. K. Charge-State Distributuion and Electric-Discharge Suppression in Negative-Ion Electrospray Mass Spectrometry Using/Chlorinated Solvents. *Rapid Commun. Mass Spectrom.* **1992**, *6* (8), 536–539. https://doi.org/10.1002/rcm.1290060811.
- (76) Ooi, T.; Uematsu, Y.; Maruoka, K. Asymmetric Strecker Reaction of Aldimines Using Aqueous Potassium Cyanide by Phase-Transfer Catalysis of Chiral Quaternary Ammonium Salts with a Tetranaphthyl Backbone. *J. Am. Chem. Soc.* **2006**, *128* (8), 2548–2549. https://doi.org/10.1021/ja058066n.
- (77) Chiu, C.-W.; Kim, Y.; Gabbaï, F. P. Lewis Acidity Enhancement of Triarylboranes via Peripheral Decoration with Cationic Groups. *J. Am. Chem. Soc.* **2009**, *131* (1), 60–61. https://doi.org/10.1021/ja808572t.
- (78) Kurono, N.; Ohkuma, T. Catalytic Asymmetric Cyanation Reactions. *ACS Catal.* **2016**, *6* (2), 989–1023. https://doi.org/10.1021/acscatal.5b02184.
- (79) Bunchuay, T.; Docker, A.; Martinez-Martinez, A. J.; Beer, P. D. A Potent Halogen-Bonding Donor Motif for Anion Recognition and Anion Template Mechanical Bond Synthesis. *Angew. Chem.* **2019**, *131* (39), 13961–13965. https://doi.org/10.1002/ange.201907625.
- (80) Turner, G.; Docker, A.; D. Beer, P. Anion Recognition by Halogen Bonding and Hydrogen Bonding Bis(Triazole)-Imidazolium [2]Rotaxanes. *Dalton Trans.* **2021**, *50* (37), 12800–12805. https://doi.org/10.1039/D1DT02414K.
- (81) Hein, R.; D. Beer, P. Halogen Bonding and Chalcogen Bonding Mediated Sensing. *Chem. Sci.* **2022**, *13* (24), 7098–7125. https://doi.org/10.1039/D2SC01800D.
- (82) Borissov, A.; Marques, I.; Lim, J. Y. C.; Félix, V.; Smith, M. D.; Beer, P. D. Anion Recognition in Water by Charge-Neutral Halogen and Chalcogen Bonding Foldamer Receptors. *J. Am. Chem. Soc.* **2019**, *141* (9), 4119–4129. https://doi.org/10.1021/jacs.9b00148.
- (83) Navarro-García, E.; Galmés, B.; Velasco, M. D.; Frontera, A.; Caballero, A. Anion Recognition by Neutral Chalcogen Bonding Receptors: Experimental and Theoretical Investigations. *Chem. Eur. J.* **2020**, *26* (21), 4706–4713. https://doi.org/10.1002/chem.201905786.

TOC graphic



A water-stable bidentate pnictogen bond donor has been evaluated for anion binding. It demonstrates very high binding affinities for cyanide, cyanate and acetate. Density functional theory calculations reveal a perfect fit for the carboxylate group. This gates the use of pnictogen bond donor systems for anion recognition and noncovalent catalysis.